Proceedings of the 5th WSEAS Int. Conf. on Artificial Intelligence, Knowledge Engineering and Data Bases, Madrid, Spain, February 15-17, 2006 (pp275-279)

A Minimal Fuzzy Entropy Model for Pattern Recognition: Evaluation in a SAR Imagery Application

V. Barrile, M. Cacciola, M. Versaci
Dipartimento di Informatica, Matematica, Elettronica e Trasporti (DIMET)
Università degli Studi Mediterranea di Reggio Calabria
Via Graziella Feo di Vito, 89100 Reggio Calabria
Italy
{barrile, matteo.cacciola, versaci}@ing.unirc.it http://www.ing.unirc.it

Abstract: - The aim of this paper is the proposition of a soft computing approach for solving patter recognition problems. In particular, starting from Shannon's Fuzzy Entropy, we propose a mathematical model which extracts fuzzy inference with minimal entropy. The proposal approach has been applied to evaluate Synthetic Aperture Radar imagery. In addition, a comparison with the classical Shannon's Fuzzy Entropy has been taken into account.

Key-Words: - Fuzzy Inference, Minimal Entropy, Synthetic Aperture Radar

1 Introduction

Pattern recognition problem is frequently approached in a lot of scientific fields. In order to solve it, various approaches have been used; at the beginning, classification tests were led by using linear classifiers (e. g. Bayesian classifier [1]), but great advantages were obtained with the introduction of nonlinear systems, such as Fuzzy Inference Systems (FIS), Artificial Neural Networks (ANNs) and Binary or Multi-Class Support Vector Machines (BSVMs and MCSVMs) [2], [3]. The main aim is to structure a handly-user pattern recognition model, sufficiently autonomous from user interferences and with good performances in terms of: reliability, robustness, computational complexity and times, as during training as during testing phases.

The aim of our work is to build a thematic map starting from a Fuzzy model by using Fuzzy Entropy Theory. In particular, a Fuzzy Entropy measure based on Shannon's informative entropy theory (i.e. Shannon's Fuzzy Entropy, SFE) has been considered, and a mathematical model able to build a pattern classifier with minimal entropy has been implemented. This is the proposed Minimal Fuzzy Entropy (MFE) classifier. It has been tested in a Synthetic Aperture Radar (SAR) context, in particular by approaching the problem of a good recognizing of punctual zones inner a SAR image, according to the specific civil or military application in which remote sensing is applied. Moreover, a comparison with usual SFE has been carried out.

The paper is organized as follows: section 2 describes mathematical fundamentals of MFE; section 3 intuitively describes SAR system as well as our case study; in section 4 implementation of MFE classifier is explained; section 5 shows a comparison between proposed approach and an usual SFE-based classifier; finally, in section 6, conclusions are depicted.

2 MFE: Decisional Models Implementation and Classification Approach

In a pattern classification problem, u_{jk} is the level of fuzzy membership of *j*th defect to *k*th class (k=1, 2, …, N). Let N classes are given, the shading-type partition produces N informative layers representing membership levels of the defects to the selected classes. Shannon index [4] has been widely applied to evaluate the fuzziness degree of a fuzzy classification. Entropy of a defect, H, i.e. its amount of statistic information, is:

$$H = -\sum_{k=1}^{N} u_{jk} \ln u_{jk} \tag{1}$$

where $\ln u_{jk} = 0$ when $u_{jk} = 0$ [5].

According to fuzzification of Shannon Entropy principle, a new SFE-based approach has been considered through construction of a Minimal Fuzzy Entropy Decisional Model (MFEDM) for each considered feature. In order to build each MFEDM, the following algorithm has been considered:

1. let us denote $X = \{x_1, \ldots, x_n\}$ as a universal set of pattern space elements, with i = 1, …, n;
2. let $\tilde{A}$ be a *k*-elements fuzzy set ($k<n$) defined on an interval of pattern space; membership degree mapping of x_i elements into the fuzzy set $\tilde{A}$ is denoted as $\mu_{\tilde{A}}(x_i)$;
3. let $C_1, C_2, \ldots, C_m$ be the *m* classes into which the *n* elements are divided;
4. let $S_{Cj}(x_n)$ represent a set of elements of j^{th} class into the universal set X;
5. let us define D_j (2), the *match degree* with the fuzzy set $\tilde{A}$ for elements of j^{th} class in an interval, where j = 1, 2, …, m:

$$D_j = \frac{\sum_{x \in S_{Cj}(x_n)} \mu_{\tilde{A}}(x)}{\sum_{x \in X} \mu_{\tilde{A}}(x)} \tag{2}$$

6. let us define SFE of elements of j[th] class in an interval, $SFE_{C_j}(\tilde{A})$:

$$SFE_{C_j}(\tilde{A}) = -D_j \log_2 D_j \quad (3)$$

7. let us define SFE in a universal set X for elements in an interval, SFE($\tilde{A}$):

$$SFE(\tilde{A}) = \sum_{j=1}^{m} SFE_{C_j}(\tilde{A}) \quad (4)$$

In (4) $SFE_{C_j}(\tilde{A})$ is a non-probabilistic entropy. Therefore, the term *match degree* for D_j has been coined. In the next section, the case study is going to be explained.

3 The Synthetic Aperture Radar

SAR is a high-resolution ground-mapping technique that effectively synthesizes a large receiving antenna by processing the phase of the reflected radar return. SAR technology is used in various technical fields, such as environmental monitoring, earth-resource mapping, and military systems, basically because two advantages:

1. application fields require broad-area imaging at high resolutions;
2. many times the imagery must be acquired in inclement weather or during night as well as day: SAR provides such a capability.

The microwave part of the electromagnetic spectrum (1-30cm) is used by radar. It was broken up into bands, listed in Table 1. For wavelengths in the region 30-75cm, the term P-band is often used. Because of atmospheric absorption effects, only certain sharply defined windows in the spectrum can be used for imaging purposes.

Table 1– IEEE names for radar frequency bands

Band	Frequency range	Wavelength range
P	0.4÷1 GHz	30÷75 cm
L	1÷2 GHz	15÷30 cm
S	2÷4 GHz	7.5÷15 cm
C	4÷8 GHz	3.7÷7.5 cm
X	8÷12 GHz	2.5÷3.7 cm

A detailed description of the theory of operation of SAR is complex; so we want to give an intuitive feel for how SAR works. Considering an airborne SAR imaging perpendicular to the aircraft velocity, SARs produce a two-dimensional (2-D) image. One dimension in the image is called range (or along track) and is a measure of the "line-of-sight" distance from the radar to the target. The along-track resolution is obtained by timing the radar return (time-gating) as for ordinary radar; in this case it has to be considered two quantities: range measurement and resolution. Range is determined by precisely measuring the time from transmission of a pulse to receiving the echo from a target; the echo's time delay is calculated as in the following equation (5):

$$t = \frac{2R}{c} \quad (5)$$

where R is the distance between radar and target. In the simplest SAR, range resolution is determined by the transmitted pulse width, i.e. narrow pulses yield fine range resolution. Considered resolution is a spatial resolution, the so called slant range resolution: considering two target points P and P', lighted up by radar beam, echoes reflected by them can be distincted if they are time-separated by an interval at least equal to the length of a transmitted impulse. Defining T_P as the impulse length, slant range resolution (Fig. 1) is calculated according to the equation (6):

$$\Delta R_s = \frac{cT_p}{2} \quad (6)$$

where division by 2 is due to the round trip of signal. Since ΔR_s e T_P are directly proportional, as smaller T_P is as greater resolution is.

Fig. 1 – Slant range resolution

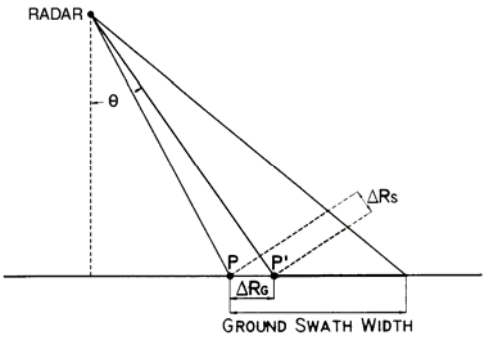

The other dimension is called azimuth (or along track) and is perpendicular to range. It is the ability of SAR to produce relatively fine azimuth resolution that differentiates it from other radars. The azimuthal resolution is obtained by processing the Doppler phase of the radar return; a physically large antenna is used to focus the transmitted and received energy into a sharp beam in order to achieve fine azimuth resolution. The beam sharpness defines the azimuth resolution.

Achieving fine azimuth resolution may also be described by a doppler processing viewpoint. A target's position along the flight path determines the doppler frequency of its echoes: targets ahead of the aircraft produce a positive doppler offset; targets behind the aircraft produce a negative offset. As the aircraft flies a distance (the synthetic aperture), echoes are resolved into a number of doppler frequencies. The target's doppler frequency determines its azimuth position. Mathematically, let us define θ_H the solid angle in which is bordered the transmitted energy and from which the system replies to received signals:

$$\vartheta_H = \frac{\lambda}{L_A} \quad (7)$$

where λ is the wavelength of transmitted energy; two target points lying on round at the same slant range distance R from radar can be distinguised only if they are not simultaneously on the same solid angle. From (7) and denoting the length of radar antenna in azimuth as L_A, it is possible to consider the azimuth resolution like (8):

$$\Delta A_Z = R \cdot \vartheta_H = \frac{R \cdot \lambda}{L_A} \tag{8}$$

Since ΔA_Z e L_A are inversely proportional, as greater the antenna length is as better the azimuth resolution is.

3.1 The Formation of SAR Images

A SAR system illuminates a scene with microwaves and records both the amplitude and the phase of the back-scattered radiation, making it a coherent imaging process.
The received signal is sampled and converted into a digital image. The field recorded at pixel x, denoted *E(x)*, can be written:

$$E(x) = \sum_s a(s) e^{i\phi(s)} h(s,x) \tag{9}$$

where the summation ranges over the scatterers, *a(s)* and *ϕ(s)* are respectively the amplitude and phase of the signal received from scatterer *s*, and *h* is the instrument (or point-spread) function. The value of *h* is near 1 when *s* is in or near the resolving cell corresponding to pixel x, and near zero otherwise. Assuming that *h* is translation-invariant (does not depend on x) then it can be written as a one-parameter function: *h(s-x)*. Thus the detected field *E* is an array of complex numbers. The square of the modulus of the field at x is called the detected intensity at x; the square-root of the intensity is called the envelope or the amplitude. This is not the same as the amplitude of the received signal because the received field is perturbed by the instrument function. The amplitude of the received signal, *a(s)*, is called reflectivity, and its square is called surface cross-section. That is what it would try to recreate when reducing the speckle. Datasets for SAR images can be stored as either intensity or amplitude data. It is important you know what type of data you are using. Many images are stored as amplitude since the speckle is less obtrusive when these images are displayed.

3.2 Case Study

In this paper, the image in Fig. 2 has been considered as case study: this is the gray-scaled version of a ERS-1 SAR multispectral survey of Torre de Hercules' coast (December 13, 1992) [6]. It was taken ten days after the disaster in which the Greek oil tanker Aegean Sea exploded at Torre de Hercules releasing all of the oil into the sea. Aircraft observations allow to conclude the very dark area is heavily polluted sea, while the dark grey area and dark streaks are older and more dispersed oil. So, it can be observed three different zones (classes) into the SAR image: Sea (S), Petroleum (PE) an Natural Terrain (NT).

Fig. 2 – ERS-1 SAR image of Torre de Hercules' coast

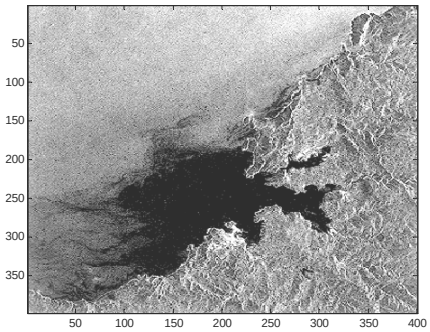

4 Implementation of MFE Classifier

In order to implement a pattern classifier, two databases are needed: one collects the pattern vectors (input database) and the other links each pattern vector **x** to its membership class. In our case, statistical quantities from first to fourth order, retrievable from the SAR image, have been considered as inputs, since it is possible to approximate the informative contents retrieved by the image with the one described by these statistical parameters. According to these considerations, **x** has four components (features): average, standard deviation, skewness and kurtosis, calculated on some sets of pixels according to the following schema:

1. first of all, some boxplots for each class have been selected on SAR image as characteristic samples of the same class (Fig. 3); each box plot is a square, which side is $l=2^n$, $4<n<7$, $n \in \mathbb{N}$;
2. let us denote S as step coefficient, initially setted to 4; inner each boxplot, all squared SxS sub-boxplots have been considered, and their statistical values have been calculated;
3. the step coefficient was multiplied by a 2 factor.

The algorithm was repeated while $S \leq l$. On the other hand, the training output database was created by using the codify shown in Table 2.

Table 2 - Codify Used to Create Output Database.

Class	Assigned label
S	1
PE	2
NT	3

Table 3 - Range of Variation of Statistical Parameters.

	Sea	Petroleum	Natural Terrain
Average	33.12÷205.94	0÷26.69	31.12÷186.19
Standard Deviation	6.81÷49.68	0÷24.75	3.3÷96.34
Skewness	-2.64÷1.99	0.2÷15.84	-2.27÷1.94
Kurtosis	1.26÷15.23	1.34÷317.36	1÷8.31

Fig. 3 – Boxplots: a) Sea, b) Petroleum, c) Natural Terrain

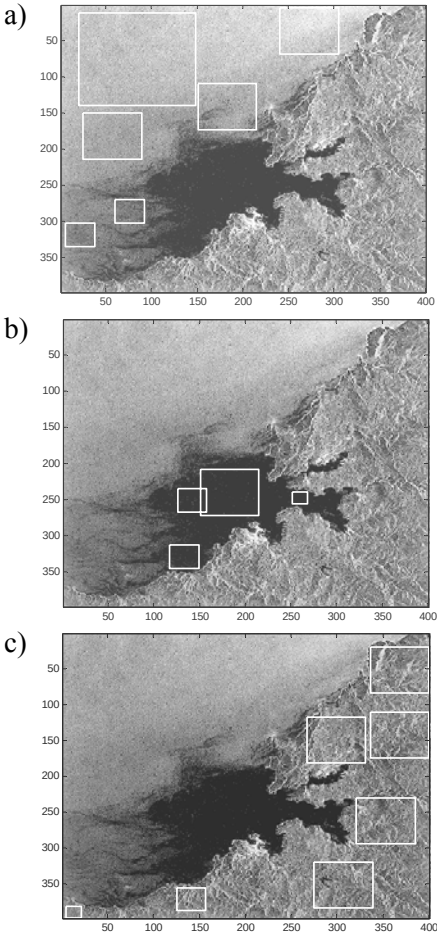

According to the mathematical algorithm proposed inner section 2, input and output databases have been used to find a MFEDM for each considered statistical parameter, in order to implement a MFE classifier. Matlab® workspace has been used, by a mixed exploiting of GENFIS® toolbox and self-made functions. Each MFEDM represents the fuzzy model which has the minimum value of entropy for a growing number of intervals (INTs), with INT initially setted to 3 (equal to number of classes in our case study). Table 4 shows INT value for each feature.

Table 4 – INT Values for Each Considered Statistical Parameter.

Mean	Std. Dev.	Skewness	Kurtosis
3	4	3	3

According to ranges showed in Table 3, each interval has been linked on each MFEDM with a triangular fuzzy membership function and an identification class. Average, skewness and kurtosis MFEDMs have a minimum of SFE corresponding to a number of intervals INT=3; standard deviation, instead, shows a minimum of SFE for a number of intervals INT=4, with PE class divided into two different intervals (Fig. 4). In this way, a MFE classifier has been implemented.

Fig. 4 – MFEDMs: a) Average, b) Standard Deviation, c) Skewness, d) Kurtosis.

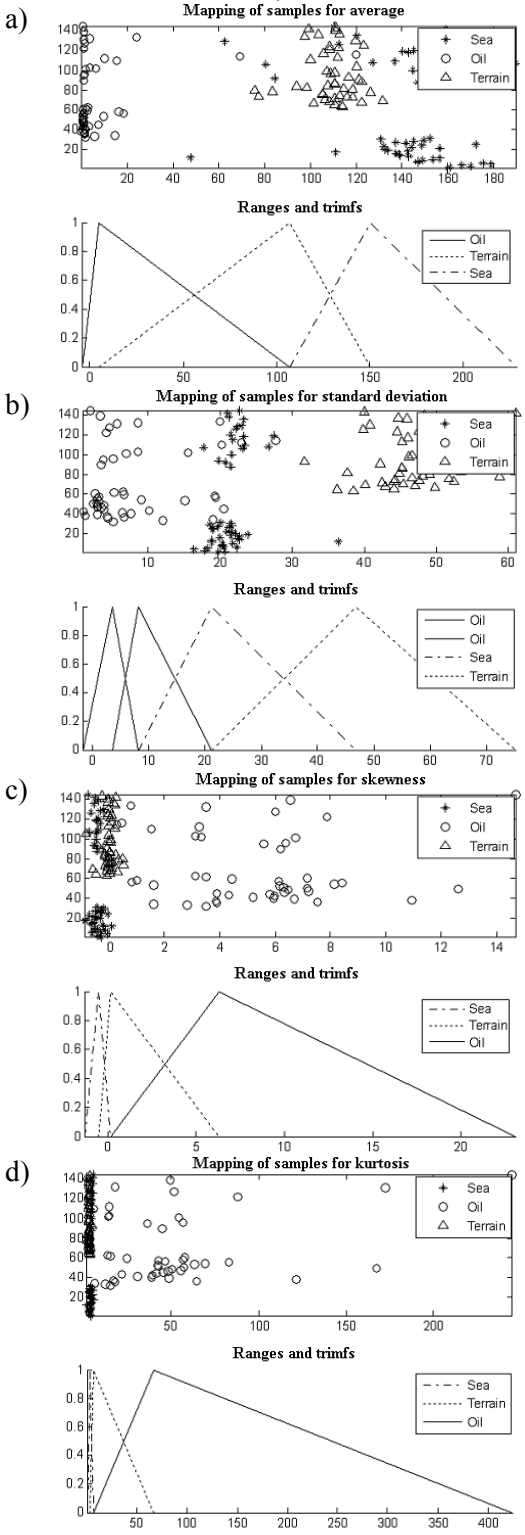

5 Comparative Test Between Usual SFE-based and MFE-based Classifiers

In order to validate proposed approach, a comparative test has been carried out between MFE classifier and one based on usual SFE principle. In spite of the image exploited is again the Torre de Hercules survey, the evaluation phase of

classifier is not invalidated. In fact, while the training database has been built by using some representative boxplots (Fig. 3), the test database has been built by using the whole image. So, even considering a mixation phase of test dataset, data appears to classifiers like a different database as regards to training one.

Since extracted features have been statistical quantities, it would be illogical to consider each pixel out of the context of the whole image. Therefore, each pixel is analyzed putting it in a window of opportune dimensions. To get an accurate estimate regarding the analyzed pixel it is necessary to have a window rather ample; but the bigger is the ampleness of this window, the higher is the probability to have a inhomogeneity inside of the same window, with a completely unreliable estimate. That's why the choice of a 9x9 pixel window has seemed quite opportune. MFE classifier, as well as SFE-based one, retrieve a new image as classification result, where:

- a white-color pixel shows a classification as Sea;
- a black-color pixel shows a classification as Petroleum;
- a gray-color pixel shows a classification as Natural Terrain.

Classification results are showed in Fig. 5; let us denote how MFE classifier has better performance than usual SFE-based one.

Fig. 5 – Classification tests: a) MFE Classifier, b) Usual SFE-based classifier.

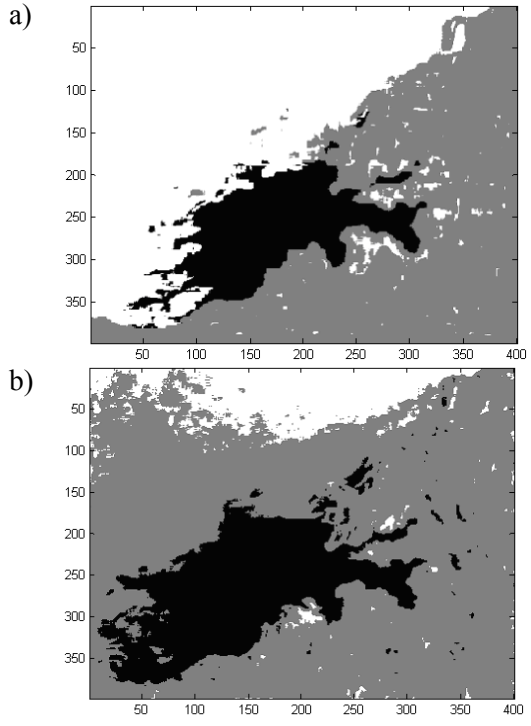

6 Conclusions

This paper presents a new Fuzzy entropy approach for pattern recognition problems. It is based on Shannon's Fuzzy Entropy, developing the principle of minimal entropy for a Fuzzy Inference System and obtaining in this way a more performing classification model. The retrieved heuristic system has been tested on a soft computing analysis of a SAR image, in order to compare its performances with ones of an usual SFE-based classifier. In this final section, by means of Fig. 5, let's go to sum up our work. As a visual analysis of Fig. 5 suggests, MFE classifier has the best performances, with a percentage of reliability around the 94%. SFE-based classifier shows a very low classification capability above all identifying the S zone; on the other hand, MFE classifier generally has very good performances, and particularly inner the band immediately over the wide oil spot, i.e. where the pollutant agent is more diffusely wasted on sea. Therefore, thanks to its "class separation" abilities, MFE classifier considers the zone as PE, with very important usefulness in such fields as environmental monitoring applications.

Finally, considering performed analyses and retrieved results, it is possible to affirm that classification machines based on MFE assure encouraging and noteworthy performances, above all when survey precision has to be privileged as regards the classification elapsed time (Table 5).

Table 5 – Comparison Between Fuzzy Classifiers.

	Visual performances	**Elapsed classification time**
MFE classifier	94%	520.22 s
SFE classifier	75%	165.83 s

References:

[1] J.J. Van Zyl and C.F. Burnette, Bayesian Classification of Polarimetric Sar Images Using Adaptive a-Priori Probabilities, *International Journal of Remote Sensing*, n. 13, 1992, pp. 835-840.

[2] Y.C. Tzeng and K.S. Chen, A Fuzzy Neural Network to SAR Image Classification, *IEEE Trans. Geosci. Remote Sensing*, n. 34, 1998, pp. 301-307.

[3] C. Huang, L.S. Davis, J.R.G. Townshend, An assessment of support vector machines for land cover classification, *International Journal of Remote Sensing*, n. 23, 2002, pp. 725-749.

[4] R.W. Hamming, *Coding and Information Theory*, 2nd ed., Prentice Hall, 1986.

[5] B. Kosko, *Fuzzy Engineering*, Prentice-Hall, Inc. Simon & Schuster/A Viacom Company Upper Saddle River, New Jersey, 1997.

[6] J. Lichtenegger, Using ERS-1 SAR images for oil spill surveillance, *ERS Data Utilisation Section, ESA/ESRIN*, Italy, available at http://esapub.esa.int/eoq/eoq44/lichten.htm (December 17, 2005).

[7] A. De Luca, S. Termini, Definition of non-probabilistic entropy in the setting of fuzzy sets theory, *Information and Control*, n. 20, 1972, pp. 301-312.